Geophys. J. Int. (2000) **142,** 755–768

Slip rate on the Dead Sea transform fault in northern Araba valley (Jordan)

Y. Klinger,[1,*] J. P. Avouac,[2] N. Abou Karaki,[3] L. Dorbath,[1,4] D. Bourles[5] and J. L. Reyss[6]

[1] *EOST, UMR CNRS-ULP* 7516, 5 rue *René Descartes,* F-67084 *Strasbourg, France*
[2] *Laboratoire de Géophysique, CEA, BP* 12, F-91680 *Bruyères le Châtel, France*
[3] *Department of Geology, Jordan University, Amman, Jordan*
[4] *IRD,* 213 *rue La Fayette,* F-75480 *Paris cedex* 10, *France*
[5] *CEREGE, Europôle Méditerranéen de l'Arbois, BP* 80, F-13545 *Aix en Provence, France*
[6] *CFR, CNRS-CEA, Avenue de la Terrasse,* F-91198 *Gif sur Yvette, France*

Accepted 2000 March 13. Received 2000 March 13; in original form 1999 April 6

SUMMARY

The Araba valley lies between the southern tip of the Dead Sea and the Gulf of Aqaba. This depression, blanketed with alluvial and lacustrine deposits, is cut along its entire length by the Dead Sea fault. In many places the fault is well defined by scarps, and evidence for left-lateral strike-slip faulting is abundant. The slip rate on the fault can be constrained from dated geomorphic features displaced by the fault. A large fan at the mouth of Wadi Dahal has been displaced by about 500 m since the bulk of the fanglomerates were deposited 77–140 kyr ago, as dated from cosmogenic isotope analysis (^{10}Be in chert) of pebbles collected on the fan surface and from the age of transgressive lacustrine sediments capping the fan. Holocene alluvial surfaces are also clearly offset. By correlation with similar surfaces along the Dead Sea lake margin, we propose a chronology for their emplacement. Taken together, our observations suggest an average slip rate over the Late Pleistocene of between 2 and 6 mm yr^{-1}, with a preferred value of 4 mm yr^{-1}. This slip rate is shown to be consistent with other constraints on the kinematics of the Arabian plate, assuming a rotation rate of about 0.396°Myr^{-1} around a pole at 31.1°N, 26.7°E relative to Africa.

Key words: Araba valley, Dead Sea fault, slip rate.

1 INTRODUCTION

Although the Dead Sea transform fault is a major plate tectonic feature, forming the boundary between the African and Arabian plates, its slip rate remains poorly constrained. The fault zone extends over 1000 km from the Red Sea rift to the collision zone in eastern Turkey (Fig. 1, inset). Its morphology is well expressed all along its strike, with several major linear stretches separated by extensional pull-apart basins, amongst which the Dead Sea Basin is the largest. Geological observations (Quennell 1956; Garfunkel *et al.* 1981) as well as plate tectonic models (e.g. McKenzie *et al.* 1970; Joffe & Garfunkel 1987; DeMets *et al.* 1994; Jestin *et al.* 1994) suggest that the Dead Sea fault accommodates the differential motion between Africa and Arabia by left-lateral slip. The modern slip rate is poorly constrained, however; geological observations suggest nearly pure strike-slip faulting and estimated rates range between 1 and 20 mm yr^{-1} (e.g. Freund *et al.* 1968; Garfunkel *et al.* 1981; Gardosh *et al.* 1990; Ginat *et al.* 1998). From the historical seismicity in the area, Ben-Menahem (1981) inferred a slip rate of about 2 mm yr^{-1}. For comparison, Nuvel1A (DeMets *et al.* 1994) predicts transpressive motion, with 7 mm yr^{-1} of left-lateral slip and 6.8 mm yr^{-1} of compression for a point located at the Dead Sea. Le Pichon & Gaulier (1988) have also proposed a slip rate of about 9 mm yr^{-1} for the Wadi Araba, based on gravimetric and magnetic data in the Red Sea. The regional plate model of Jestin *et al.* (1994) was forced to accommodate 1 cm yr^{-1} of pure strike-slip faulting along the Dead Sea fault.

Numerous authors have described the fault zone along the Araba valley between the southern end of the Dead Sea and the Gulf of Aqaba (Garfunkel *et al.* 1981; Bowman & Gross 1992; Bowman 1995). It cuts the alluvial floor of the rift valley sharply along a particularly straight trace striking N20°E

* Now at: Seismological Laboratory, Mail stop #100–23, California Institute of Technology, Pasadena, CA 91125, USA. E-mail: yann@gps.caltech.edu

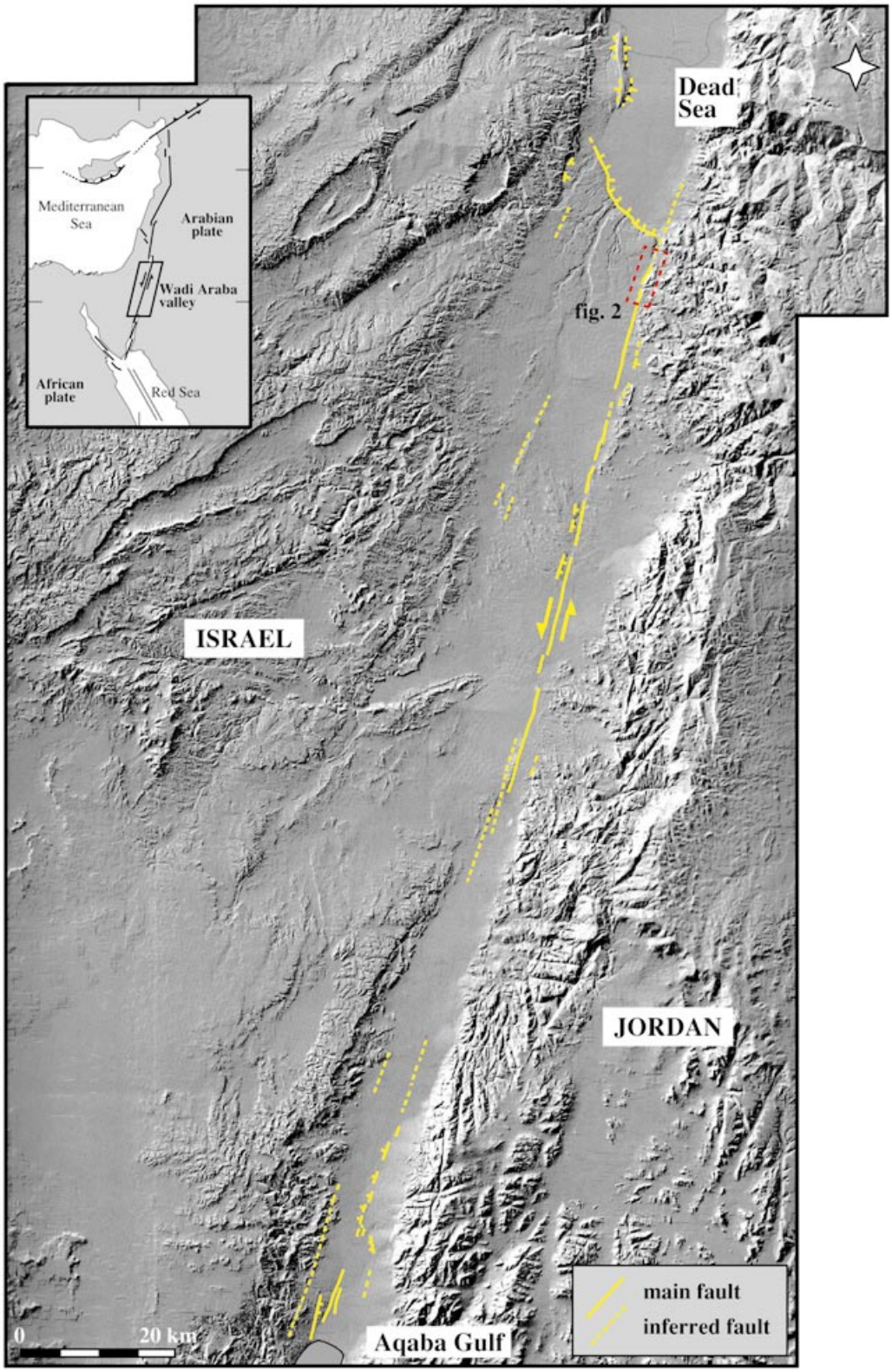

Figure 1. Active faults of Wadi Araba modified from Garfunkel *et al*. (1981) on the basis of air photos together with SPOT and Landsat images. Only faults affecting Quaternary surfaces have been mapped. DEM adapted from Hall (1994). Box shows location of Fig. 2 and inset depicts regional tectonic setting.

(Fig. 1). The fault's geometry at the surface is relatively simple, with only a few subsidiary faults. This area is thus particularly favourable for allowing the determination of the slip rate from offset geomorphic features such as displaced alluvial fans or terrace risers (e.g. Peltzer *et al*. 1989; Harden & Matti 1989). This approach generally suffers from the difficulty of dating such features, in particular because organic material is rare in this arid environment. We have taken advantage of the new

possibilities offered by cosmogenic dating (e.g. Molnar *et al.* 1994; Ritz *et al.* 1995; Brown *et al.* 1998) and of the relatively well-constrained chronology of the geomorphic evolution near the Dead Sea margin and its relation to lake level variations (Klein 1982; Begin *et al.* 1985; Frumkin *et al.* 1991; Yechieli *et al.* 1993; Klinger 1999).

We first summarize the tectonic background and the geomorphic and sedimentological setting of the Wadi Araba valley. Next we focus on the Dahal alluvial fan (see box in Fig. 2), which is a particularly outstanding example of an offset geomorphic feature along the Wadi Araba segment of the Dead Sea fault. We then discuss younger terraces that also show clear

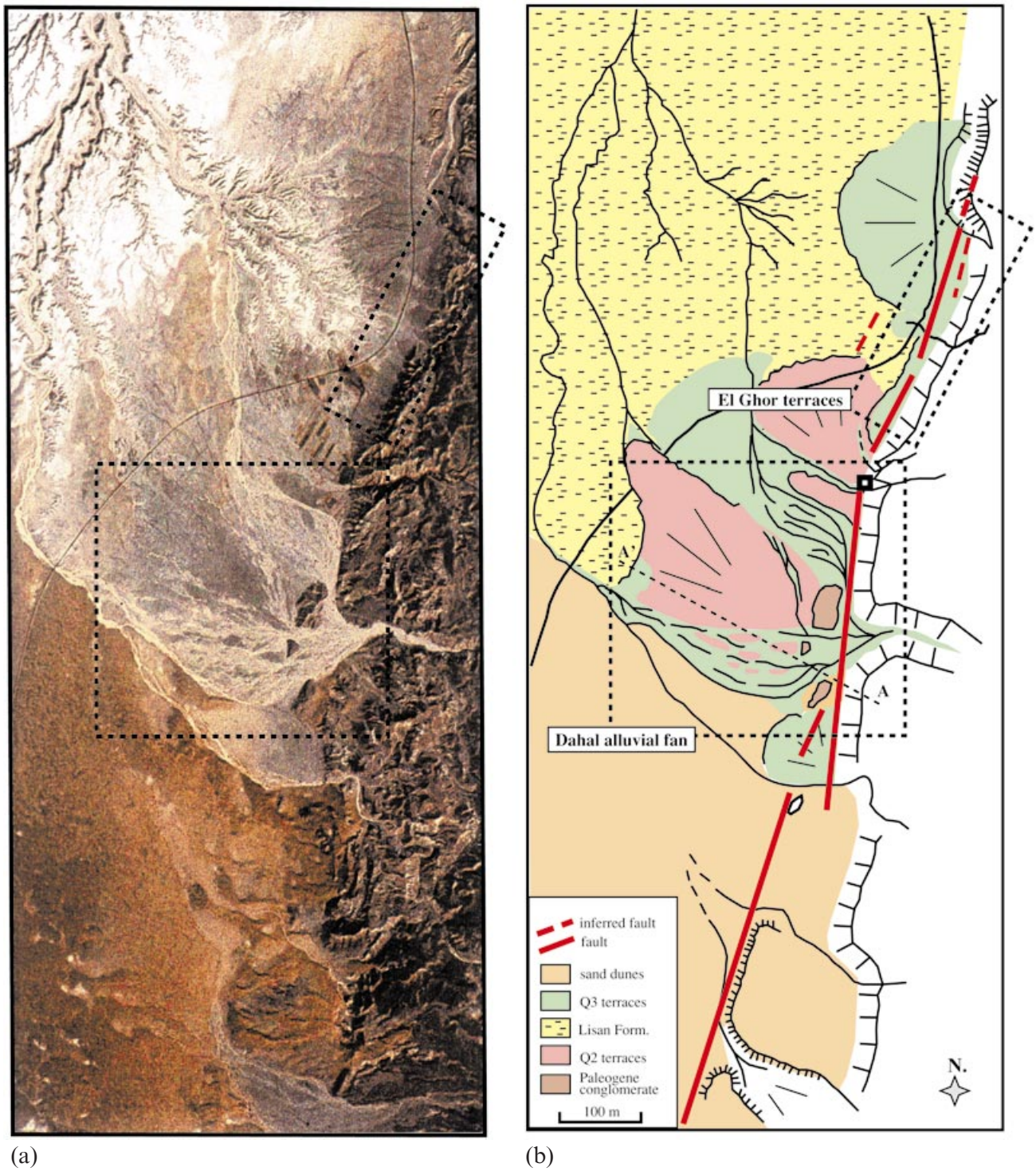

Figure 2. (a) SPOT panchromatic image of the northeastern Wadi Araba. See Fig. 1 for location. (b) Schematic geological and geomorphological setting of the area. The fault zone is located in between the mountain front and the Dahal alluvial fan. The location and shape of the Q2 terrace (see topographic contour lines in Fig. 4) suggest that Q2 terraces have been offset left-laterally by the fault since its deposition. Box shows location of Fig. 4.

offsets (the El Ghor terraces in Fig. 2). Finally, we derive the slip rate on that particular segment of the Dead Sea fault and discuss its consistency with other constraints on the kinematics of the Arabian plate.

2 MORPHOTECTONIC BACKGROUND

The Dead Sea fault is considered to be a major strike-slip fault that has accommodated about 100 km of cumulative left-lateral slip (e.g. Quennell 1956; Garfunkel *et al.* 1981), probably after to the reorganization of regional tectonics that took place about 15 Myr ago (Courtillot *et al.* 1987). Along Wadi Araba, the fault trace is particularly sharp and straight across the alluvium. It is associated with very little relief except locally at small compressional or extensional jogs (Fig. 1). This geometry suggests pure strike-slip faulting, as already inferred by previous investigators (e.g. Garfunkel *et al.* 1981). The fault pattern becomes more complex where it connects with the two large regional pull-apart basins of the Dead Sea in the north (e.g. Ten Brink *et al.* 1993) and the Gulf of Aqaba in the south (e.g. Ben-Avraham 1985).

Due to Neogene extension (Freund *et al.* 1968), the Dead Sea fault zone is marked by a conspicuous rift valley, which is particularly well expressed along the Araba valley (Fig. 1). The rift flanks are still high, even though considerably smoothed by erosion. The alluvium in the rift valley mainly consists of fanglomerate fed from the ephemeral rivers incising the rift flanks. Locally, extensive dune fields cap the fans (Figs 1 and 2). The fans are relatively flat and their lateral merging has formed a continuous piedmont with little relief. The alluvial surfaces in the region are generally subdivided into three groups, depending on their relative position, degree of desert pavement and weathering (e.g. Grossman & Gerson 1987). Upper terraces are Pleistocene surfaces. They are characterized by a well-developed varnish on their surfaces and a smooth desert pavement with weathered boulders and pebbles. Lower terraces are Holocene surfaces characterized by a well-preserved bar and swale morphology, a poorly developed desert pavement, a poor varnish development and a low to moderate degree of weathering of exposed gravels. Active floodplains are characterized by braided channels and show neither a desert pavement nor a varnish. These different surfaces can be distinguished on satellite images and aerial photography (Fig. 2). The well-developed desert pavement and varnish on the Pleistocene surfaces result in a dark chromatic signature (Fig. 2). Zones of recent or active wash are bright and Holocene surfaces are intermediate. Along Wadi Araba, the various surfaces lie at similar elevations and well-preserved Pleistocene surfaces are abundant. This suggests that no large aggradational episode has occurred since the Pleistocene terraces were abandoned, nor has there been much vertical motion. This is in keeping with pure strike-slip faulting along the Wadi Araba fault.

At the southern tip of the Dead Sea, alluvial surfaces merge with extensive outcrops of yellow–white lacustrine sediments, the Lisan Formation, that were deposited during periods of highstands of Lake Lisan, the palaeo-Dead Sea lake in the Late Pleistocene (Kaufman *et al.* 1992; Druckman *et al.* 1987). The fluctuations of the Dead Sea lake during the Late Pleistocene and Holocene periods are, moreover, relatively well known from various studies combining archaeological, geomorphic and sedimentological information (Klein 1982; Begin *et al.* 1985; Frumkin *et al.* 1991; Frumkin *et al.* 1994; Klinger 1999). The area is thus particularly interesting because the timing of alluvial aggradation may be in part constrained from the relationships with well-dated lacustrine sediments and shore features.

3 AGE OF GEOMORPHIC FEATURES IN THE STUDY AREA

In this section we discuss the various geomorphic surfaces in the study area and their assigned ages. The chronological framework is based on new age control, and on a compilation of various data from the literature. This material is discussed in more detail by Klinger (1999).

Due to the degree of weathering and desert varnish development, the oldest alluvial surfaces in the study area form dark patches that are preserved adjacent to active washes on the Dahal alluvial fan (Q2 in Fig. 2). This surface mainly consists of strongly weathered pebbles of limestone and chert that range from 20 to 40 cm in size. The desert pavement is not well developed due to episodic cover by aeolian deposits. In order to place some bounds on the age of this surface, we sampled chert pebbles on the fan surface and measured their content of *in situ*-produced cosmogenic ^{10}Be. *In situ*-produced cosmogenic nuclides result from nuclear interactions between cosmic rays and the constituents of superficial rocks, and their concentration is therefore representative of the length of time that the sample has been lying at the surface. The age of a given sample may not really be representative of the age of the geomorphic surface, however. A sample may have been exposed to cosmic rays before its latest deposition. In that case its cosmogenic age overestimates the true age of the geomorphic surface. The opposite may also happen. For example, a sample may have been recently deposited long after the deposition of the bulk of the alluvium, or it may have been partly shielded from cosmic radiation because it was brought to the surface due to denudation of the surface (for a more complete discussion of those problems, the reader is referred to Cerling & Craig 1994). In the present study, we have sampled pebbles that are as large as possible that were partially embedded in the fan. Four samples were collected on the surface and one at a depth of 60 cm (DAHAL8). The apparent age of the pebbles can be interpreted as minimum exposure times. They range from 32 ± 7 kyr to 140 ± 31 kyr. This wide range of *in situ*-produced ^{10}Be concentration of the surficial samples indicates that they have experienced different depositional histories. However, when corrected for sampling depth using a density of 2 g cm^{-3} for the overlying material, the *in situ*-produced ^{10}Be concentration measured for DAHAL8 corresponds to a surficial exposure age of 140 ± 31 kyr, which is remarkably similar to the oldest age obtained from the surficial samples. In the case of post-depositional processes that are generally not uniform across a fan surface, the oldest age in the distribution is generally interpreted as closest to the true age (Brook *et al.* 1993). Hence, the similarity in ages strongly suggests that the observed dispersion most likely results from post-alluvial fan surface abandonment processes rather than significant exposure prior to deposition, although this cannot be completely ruled out.

The age of Q2 can also be constrained from the stratigraphic relationships with the lacustrine units that crop out at the toe of the fan surface (Fig. 2). From field investigation of

stratigraphic sections exposed along deeply incised gullies, we observed that the lacustrine sediments are transgressive onto the buried Q2 surface. The contact is marked by a break in slope in the topography that can be observed at an elevation of about 180 m below sea level (bsl) (Fig. 3). The gravel beds can be traced beneath the overlapping, fine-grained, well-laminated and aragonite-rich lacustrine sediments. These sediments have all the characteristics of the Lisan Formation, which is known to have been deposited from 70 to about 15 kyr ago (Begin *et al.* 1974; Kaufman *et al.* 1992). We collected two samples rich in aragonite, DAHAL9 at an elevation of about 200 m bsl and DAHAL10 at an elevation of about 190 m bsl, that were datable using the U/Th method. The radiochemical procedure used for thorium and uranium isotope separation was similar to that described by Ku (1976), using a $^{232}U/^{228}Th$ spike. Alpha counting was carried out either in a grid chamber or with a solid-state detector. Errors are expressed as 1σ based on counting statistics. The highest sample, DAHAL10, yielded an age of 26 ± 1.8 kyr, whereas the lowest, DAHAL9, yielded an age of 31.5 ± 2 kyr. These two ages are consistent with their stratigraphical positions and with the ages reported by Kaufman *et al.* (1992) for the Lisan Formation. We conclude that the oldest terrace on the Dahal fan, Q2, was abandoned in the Late Pleistocene, certainly after 140 kyr BP and before 32 kyr BP. Given that the Lisan period of deposition is considered to coincide with minor aggradation (Sneh 1979), the Dahal fan was probably mostly built up before the Lake Lisan transgression, possibly during the major aggradational episode that is described regionally (Horowitz 1987; Zilberman 1993) and that may well be associated with the last interglacial period. Hereafter we will assign an age range to Q2 of 70–140 kyr BP. Our preferred scenario is that the bulk of the fanglomerate was deposited during the last interglacial around 120 kyr BP.

Lake Lisan reached its maximum level in the Late Pleistocene–Early Holocene at about 15 kyr BP and dropped rapidly after about 12 kyr BP (Begin *et al.* 1985). The lake regression was accompanied by entrenchment of all the stream channels around the Dead Sea margin (Sneh 1979; Bowman 1988). A thin gravel veneer is described regionally and is observed to cap the uppermost Lisan sediments (Q3a in Fig. 3) (e.g. Bowman & Gross 1992). This gravel sheet probably marks the change to more arid conditions at the end of the lacustrine period and may be assigned an age of between 15 and 12 kyr BP, just before a return to wetter conditions (e.g. Begin *et al.* 1985). From the observation of fan terraces inset into the Lisan fan deltas along the Dead Sea margin, we found evidence for only two major episodes of fan aggradation in the Holocene period (Q3b and Q3c) (Klinger 1999). We are able to constrain the age of these two episodes from radiocarbon dating of organic material from the elevation of shore features that mark the Holocene Dead Sea lake transgressions. The terrace Q3b must have been emplaced between 8800 and 5200 yr BP, with a preferred range between 7000 and 6200 yr BP. The youngest terrace, Q3c, was deposited between 4400 and 2010 yr BP, most probably after the lake transgression dated at 3400 yr BP [a more detailed discussion is given in Klinger (1999)].

4 OFFSET OF THE LATE PLEISTOCENE DAHAL FAN

The Dahal alluvial fan is one of the major fans in the northern Araba valley. Its feeding river, Wadi Dahal, drains one of the largest basins in the area, with a catchment of over 7 km^2. Given its size, this fan is not comparable with the smallest fans in the area, which are easily reshaped during each severe flash

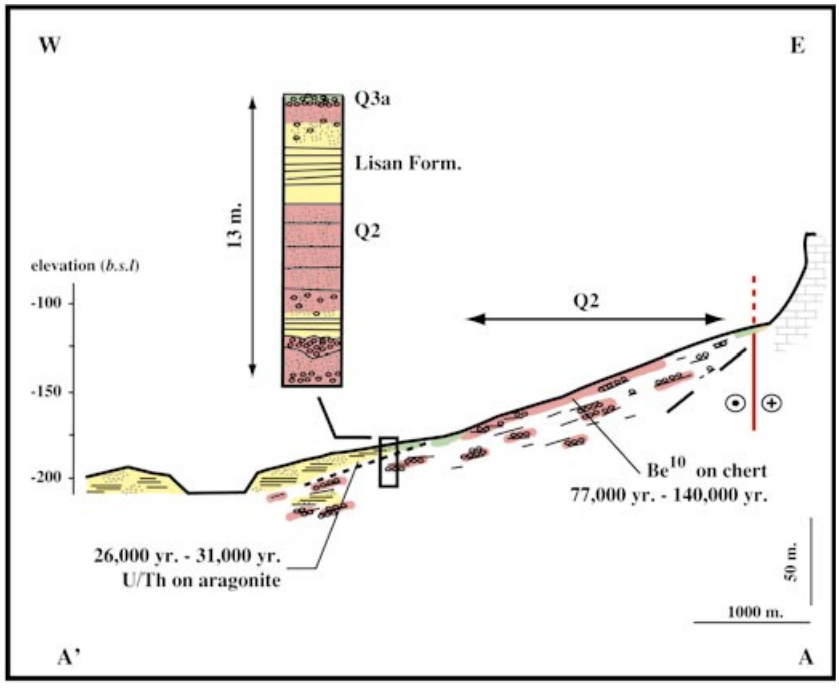

Figure 3. Summary cross-section of Dahal alluvial fan along profile A–A′ (see Fig. 2 for location). The break in slope clearly indicates the overlapping of the Lisan Formation on the Dahal alluvial fan. The interfingering of the Q2 formation and the Lisan formation at the toe of the fan shows that the fan could have still been active when the transgression of the Lisan formation started. Vertical exaggeration is $\times 8$. Colours correspond to the units in Fig. 2.

flood. Given that the fault trace cuts the apex of the fan, it is situated in a particularly favourable position to have recorded fault slip (Harden & Matti 1989). As seen on the satellite SPOT image, the fault can be traced along the topographic scarp, which mainly consists of Upper Cretaceous limestone (Quennell 1955) (Fig. 2). There are no other conspicuous strike-slip faults in the area, so we infer that most of the motion across the Dead Sea fault zone must take place on that particular fault trace.

The canyon cut by Wadi Dahal in the rift flank is relatively linear and reaches the fault immediately in front of a small ridge composed of well-indurated Palaeogene conglomerate (Figs 2 and 4). The active drainage is diverted abruptly northwards along the fault trace. This geometry, together with the observation that Holocene terraces were deposited systematically north of the Q2 fan terraces (Fig. 2), suggests that slip must have occurred along the fault since Q2 deposition. Such a shingling arrangement of the successive fan lobes is indeed a common characteristic of fans offset by strike-slip faulting (Mastalerz & Wojewoda 1993).

The topographic map of the area shows that the preserved patches of Q2 alluvium show a relatively well-defined fan shape geometry (Fig. 4). The position of the apex of the fan at the time of Q2 emplacement may thus be estimated. To do so, we have assumed a conical geometry built on an ellipsoidal base (Bull 1964; Troeh 1965; Blair & McPherson 1994). Theoretical contour lines (red lines in Fig. 4) were fitted to the observed ones: for each point that defines the observed contour lines we compute the theoretical corresponding point, according to the assumed geometry of the fan. The parameters of the theoretical fan have been tuned to minimize the difference between theoretical and observed points following an iterative scheme. The position of the best-fitting apex (red cross in Fig. 4) lies 500 m south of the mouth of the Wadi Dahal canyon. Assuming that the Q2 fan was deposited over a relatively short period of time about 120 kyr ago, this measurement would imply 500 m of cumulative offset, and hence an estimated slip rate of about 4 mm yr^{-1}. The construction of the Dahal fan was probably not that short, however. We may nevertheless

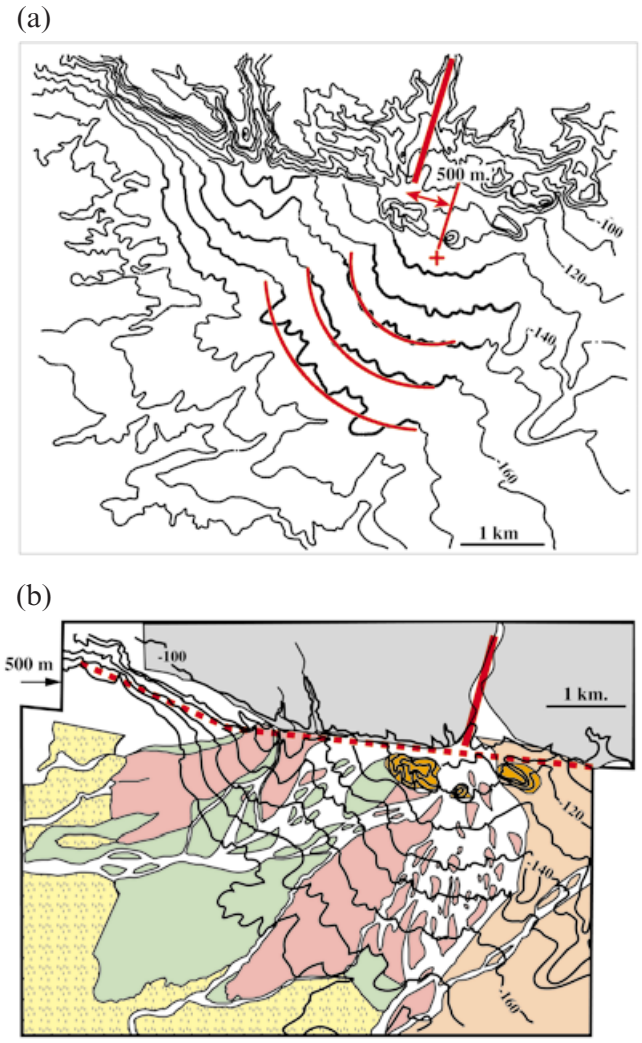

Figure 4. (a) Close-up view of the topography of the Dahal alluvial fan. The red lines are theoretical contour lines that best fit the topographic contour lines, assuming a conical shape. For the modelling we only consider the contour lines that are clearly associated with the Q2 surface. The red cross shows the location of the apex of the modelled fan derived from the geometry of the contour lines on Q2. The thick red bar follows the canyon incised by Wadi Dahal in the rift flank. The apex of the fan, according to the modelling, lies about 500 m south of the mouth of its feeding river, suggesting 500 m of left-lateral offset since Q2 deposition at about 120 kyr BP. (b) Restored geometry at the time of Q2 deposition. Topography is from the Jordanian 1:50 000 topographic map. Colours correspond to the units in Fig. 2.

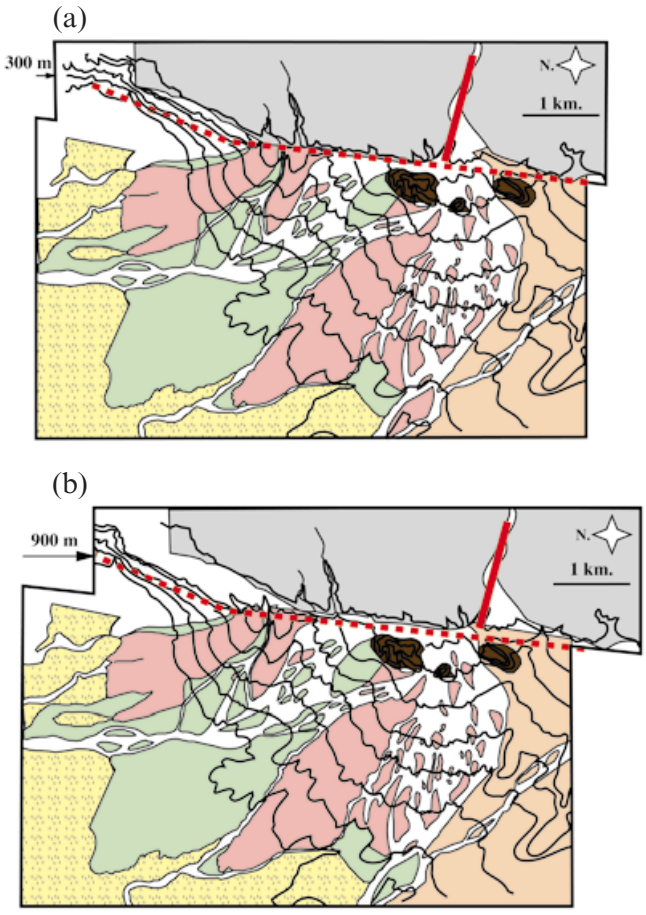

Figure 5. According to the geometry of the Q2 terrace, the Wadi Dahal was flowing straight across the shutter ridge composed of Palaeogene conglomerates during the emplacement of Q2. From that it is possible to infer restorations corresponding to minimum (a) and maximum (b) offsets, respectively, of 300 and 900 m for the Q2 surface.

contend that as long as Wadi Dahal was still aggrading significantly, it was able to maintain a fairly conical geometry due to channel avulsion at the fan surface, with an apex always in front of the mouth of the Wadi Dahal canyon. The 500 m offset would therefore be representative of the cumulative slip since Q2 abandonment. On the basis of our age determinations discussed above, a minimum age for that abandonment is 32 kyr BP, but it most probably took place before Lake Lisan transgression at about 70 kyr BP.

In order to place bounds on the slip rate we must also take into account the uncertainty on the determination of the offset. We may assume that at the time Wadi Dahal was aggrading the Q2 deposit; it was probably cutting straight ahead across the Palaeogene hills that now form a shutter ridge. Other configurations with an apex located in between the hills and the mountain front would have forced the wadi to spill around the hills and to build two distinct fans, or at least a composite fan, which is not observed. The restoration in Fig. 5(a) indicates a minimum slip of about 300 m. Given that Q2 was abandoned probably after 140 kyr BP, it yields a minimum slip rate of 2.1 mm yr^{-1}. From the other conglomerate ridge that is lying further south, we obtain a maximum slip of 900 m, as shown in

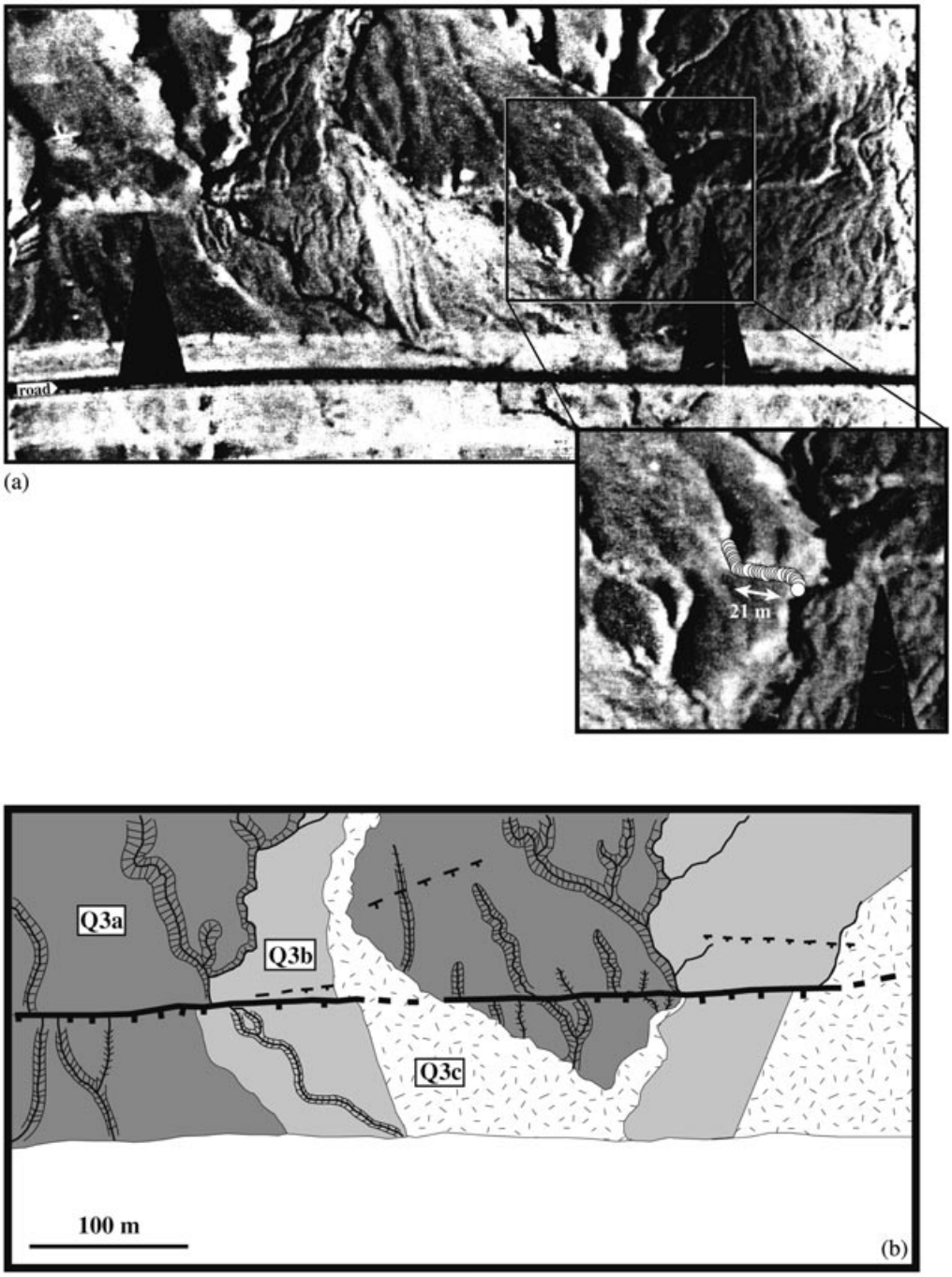

Figure 6. (a) Air photos of the fault zone across the El Ghor terraces, modified from Bowman (1995). Inset shows close-up view of an offset gully that was also measured in the field with the total station (superimposed dots show measurement points). (b) Morphotectonic interpretation showing the three terraces Q3a, Q3b and Q3c and the fault zone. In both (a) and (b) gullies are visible abutting the fault scarp.

Fig. 5(b). Assuming a post-Lisan Q2 aggradation we obtain a maximum rate of 12 mm yr^{-1}. In the following we try to check and refine this estimate from the analysis of younger morphologic offsets.

5 OFFSET OF HOLOCENE GEOMORPHIC FEATURES IN THE EL GHOR AREA

Just north of the Dahal fan, the fault cuts across younger terraces (see box in Fig. 2). As already noted by Bowman (1995), the fault trace is particularly clear in the morphology (Fig. 6). Due to a slight change in the fault azimuth, the fault pattern becomes more complex, with several subsidiary faults. Actually, only the major fault trace shows evidence for strike-slip motion. This fault also accommodates a dip-slip component that has produced a scarp up to 1.5 m in height, but the strike-slip motion is clearly dominant. Numerous gullies and terrace risers incised into the various terraces are cut and offset several metres by the fault. Fig. 6(a) shows a clear example of an offset gully, which was also measured in the field using a geodetic total station, a combination of a theodolite and a distance-ranging device. The profile indicates an offset of 21 ± 1 m (Fig. 6a, inset). Below we first describe the alluvial terraces and their ages.

5.1 Description of the terraces

The alluvial pediment consists mainly of limestone pebbles with some chert and basalt. Three terraces can be distinguished (Fig. 6). The highest one exhibits a smooth bar and swale

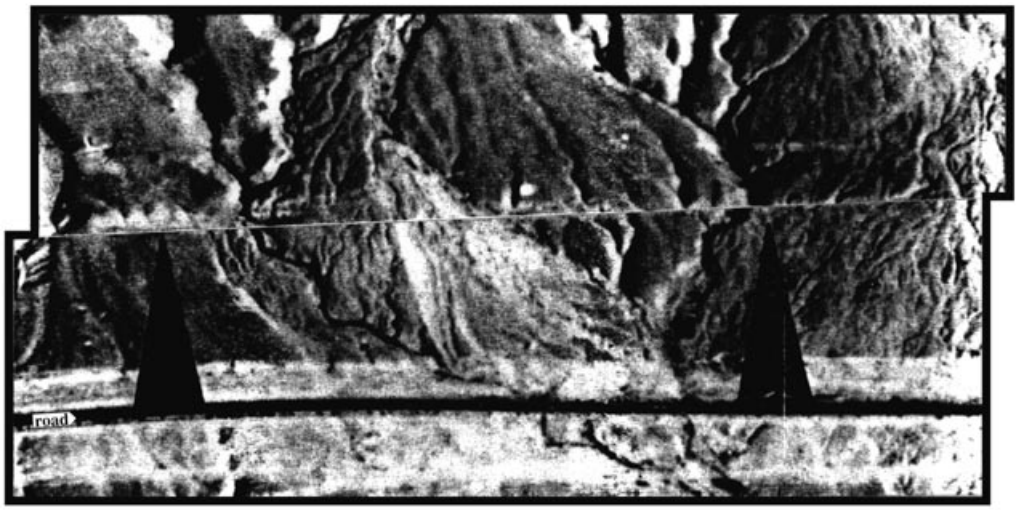

(a)

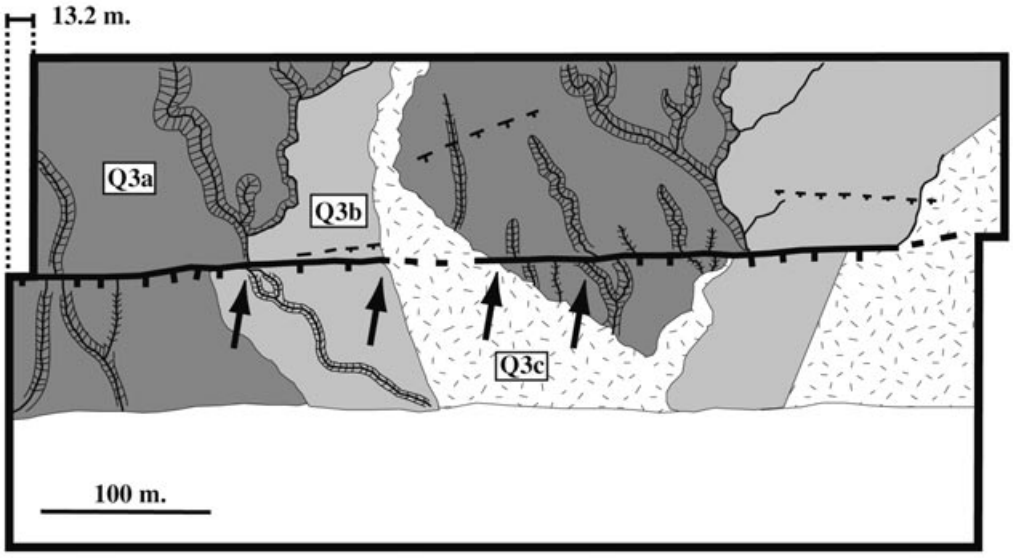

(b)

Figure 7. A reconstructed air photo (a) and interpretative sketch (b) corresponding to 13.2 m of slip. Arrows point to the incised gullies and terrace risers that are matching across the fault when we consider 13.2 m of back-slipping. Since the Q3c fan surface is restored to its initial geometry, the 13.2 m offset is necessarily younger than the emplacement of the Q3c fan.

morphology. It is paved with slightly varnished pebbles, resulting in a relatively dark colour on the air photos. It grades downslope into a gravel veneer capping the top of the Lisan Formation (Fig. 2). We therefore label this terrace Q3a and assign it an age of between 15 and 12 kyr BP. The two other terraces are inset into Q3a. They are characterized by a rougher topography and pebbles with negligible varnish. Assuming that they correlate with the Q3b and Q3c terrace levels that are systematically observed around the Dead Sea margin, they are assigned periods of deposition between 7 and 6.2 kyr BP and 3.4 and 2.1 kyr BP, respectively (Klinger 1999). In the absence of any direct dating, the rationale for this correlation is the assumption that river entrenchment and terrace deposition were forced essentially by climatic fluctuation. Such an assumption is often made when no direct dating is available, as in this case (Peltzer *et al.* 1988, 1989; Molnar *et al.* 1994; Gillespie & Molnar 1995).

5.2 Displacements on the El Ghor segment

The various gullies that flow across the fault trace are clear on the eastern side of the fault because they have incised the fault scarp. Some of them abruptly abut the fault trace and some are deflected due to left-lateral offset. The fault trace therefore marks a sharp morphological discontinuity.

We have tried to reconstruct originally contiguous morphological features by restoring (back-slipping) the motion on the fault. As shown in Fig. 7, we first reconstructed 13.2 m of slip to realign the risers separating Q3b and Q3c on one side and Q3a and Q3c on the other side as straight and linear features. If our reconstruction is correct, this suggests that about 13.2 m of left-lateral slip has occurred since emplacement of the Q3c terrace. Some offset gullies are also restored as continuous features, supporting our reconstruction. This observation suggests an episode of local aggradation of Q3c nearly coeval with

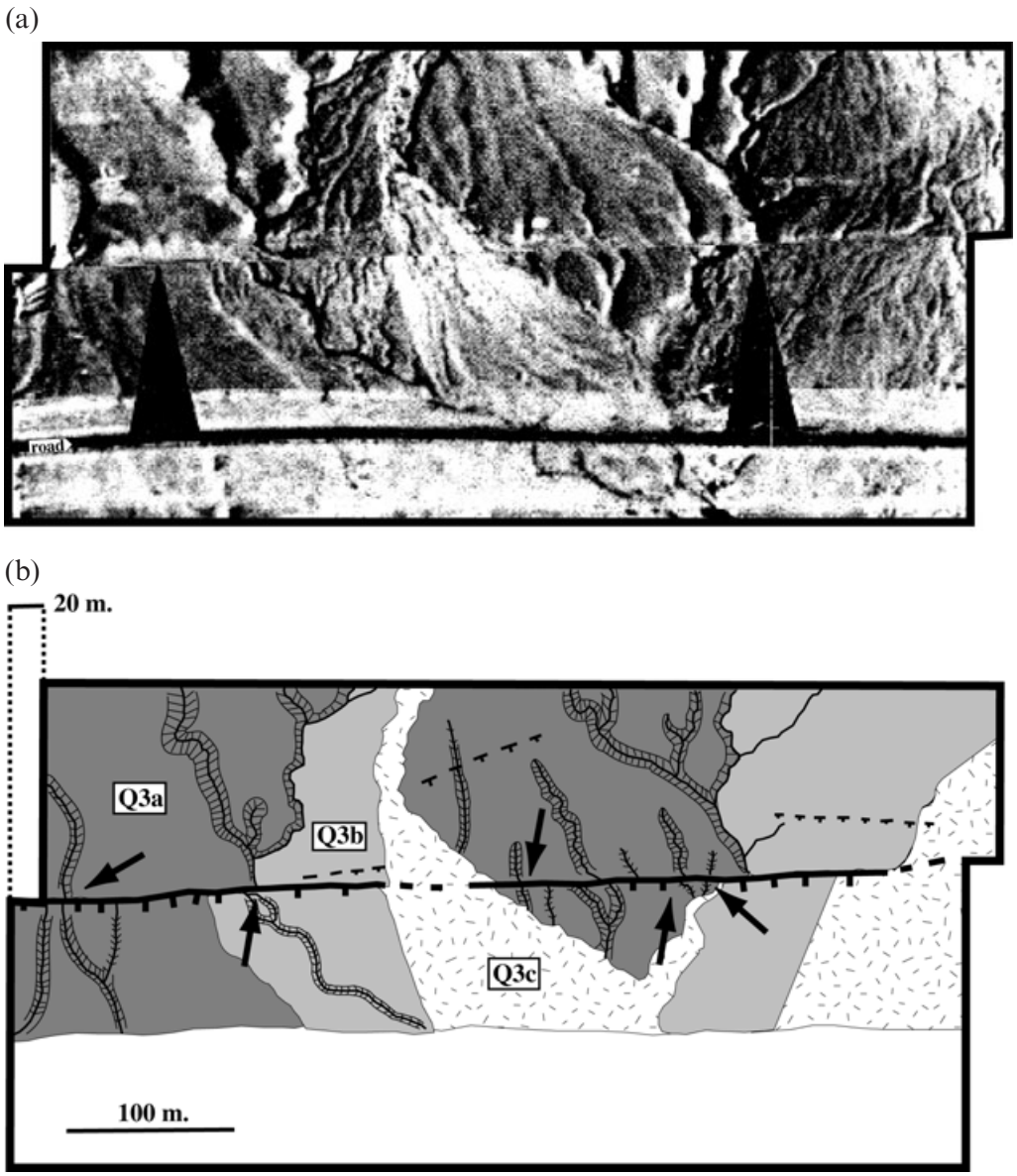

Figure 8. A reconstructed air photo (a) and interpretative sketch (b) corresponding to 20 m of slip. Arrows point to the incised gullies and terrace risers that are restored by 20 m of reconstruction. The matching of the gully incised in Q3b indicates that the offset of 20 m post-dated the deposition of Q3b.

an episode of gullying. This would be consistent with the view that, as proposed by Bull (1991), an aggradation episode in an arid environment generally ends with an episode of entrenchment. By comparing with field measurements, we estimate the uncertainty on the offset to be about 1 m. We conclude that 13.2 ± 1 m of slip has taken place since 2–4.2 kyr BP, and after 2–3.4 kyr BP if we adopt our preferred chronological scenario. This yields a Late Holocene slip rate of 2.9–7.1 mm yr^{-1}, with a preferred rate of 3.8–6.1 mm yr^{-1}.

Fig. 8 shows another configuration that also restores several geomorphic offsets. It corresponds to about 20 ± 2 m of slip. One gully is clearly incised into Q3b, so that this slip is probably younger than Q3b emplacement, and therefore younger than 8.2 kyr BP. If we consider that the episode of gullying marks the end of Q3b deposition, we may assign it an age of deposition between 7 and 6.2 kyr BP if we adopt our preferred scenario. This yields a minimum early Holocene to present slip rate of 2.6–3.5 mm yr^{-1} if our age assignments are correct, because the incision must have occurred after Q3b deposition.

It may be seen in Fig. 8 that some gullies seem to have recorded still larger offsets. Fig. 9 shows a reconstruction corresponding to 36 m of slip. Several major gullies incised into Q3a are relatively well restored, suggesting that 36 ± 2 m of

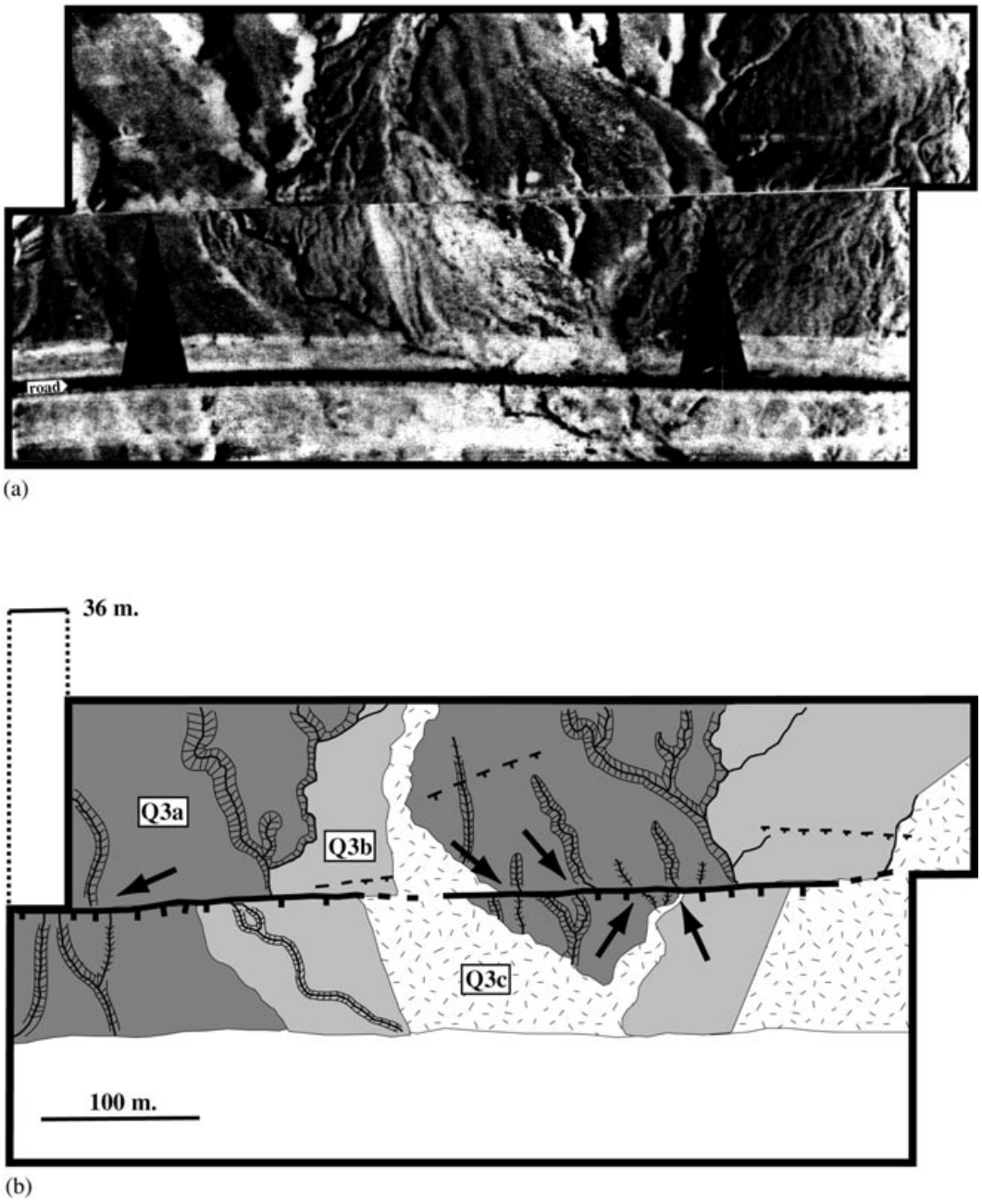

Figure 9. A reconstructed air photo (a) and interpretative sketch (b) corresponding to 36 m of slip. Arrows point to the incised gullies and terrace risers that are restored by 36 m of reconstruction. The matching of the gully incised in Q3a indicates that the offset of 36 m post-dated the deposition of Q3a.

cumulative slip must have occurred after Q3a deposition. Using the 12–15 kyr age inferred for the Q3a deposits, and again assuming that the incision occurred soon after deposition, a minimum Late Pleistocene slip rate of about 2.3–3.1 mm yr^{-1} is inferred.

6 DISCUSSION

At the El Ghor site, we have presented evidence for at least 36 m of slip since Q3a deposition, and it seems that three major episodes of alluviation are recorded in the morphology and more or less correlate with Q3a, Q3b and Q3c emplacement. Although very tentative, the proposed chronological framework can be used to test the consistency with the cumulative slip derived from the Q2 fan terrace on the Dahal fan. Fig. 10 is a plot of all measured offsets as a function of their assigned ages. Two chronological assignments are shown. Shaded boxes correspond to our preferred scenario. The dashed boxes correspond to looser constraints. It shows that an average slip rate of 4 mm yr^{-1}, corresponding to about 500 m of offset since the last interglacial period, is roughly consistent with all the data discussed above. A slip rate smaller than about 2 mm yr^{-1}, or larger than 6 mm yr^{-1}, seems improbable.

This study confirms the range of 3–7.5 mm yr^{-1} proposed by Ginat *et al.* (1998) from the offset Plio-Pleistocene alluvial terraces further south in the Wadi Araba. It also seems to be consistent with preliminary GPS measurements north of the Dead Sea, which yield about 4 mm yr^{-1} (Pe'eri *et al.* 1998).

We also checked the consistency with other data that put constraints on the motion of the Arabian plate. Fig. 11 shows various poles of rotation of Arabia with respect to Africa determined either from global plate kinematics or from regional models (Table 1). Considering the few quantitative data available, Sinai and Africa have been considered as the same plate. None of these poles fits satisfactorily with 4 mm yr^{-1} of pure strike-slip motion on the Dead Sea fault along Wadi Araba (Fig. 11, Table 3). In order to check whether our data can be reconciled with regional kinematics we have tried to adjust the motion of the Arabian plate. To do this we have also considered other kinematic data, which are listed in Table 2. They include GPS data in northern Arabia (Reilinger *et al.* 1997; Pe'eri *et al.* 1998), SLR data in Israel (Smith *et al.* 1994) and the extension across the Asal Rift at the boundary between Arabia and Somalia (DeChabalier & Avouac 1994). All the velocities are expressed with respect to Africa, and a random search method has been used to find an Eulerian pole that can account for both directional and velocity measurements (Table 2). It turns out that all the data can be fitted satisfactorily using a Eulerian pole that does not differ significantly from previous determinations (Table 1). This test demonstrates that our revised estimate for the slip rate on the Dead Sea fault of 4 ± 2 mm yr^{-1} remains consistent with the relative motion between Arabia and Africa as constrained from other techniques.

Table 1. Modern poles of rotation for Arabia relative to Africa. Rotation is positive counterclockwise.

Latitude °N	Longitude °E	ω (° Myr^{-1})	Reference
24.00	24.10	0.400	DeMets *et al.* (1994)
32.59	23.70	0.418	Jestin *et al.* (1994)
21.60	20.03	0.340	Reilinger *et al.* (1997)*
30.10	26.70	0.396	this study

*Transposed to Arabia/Africa using Nuvel1A.

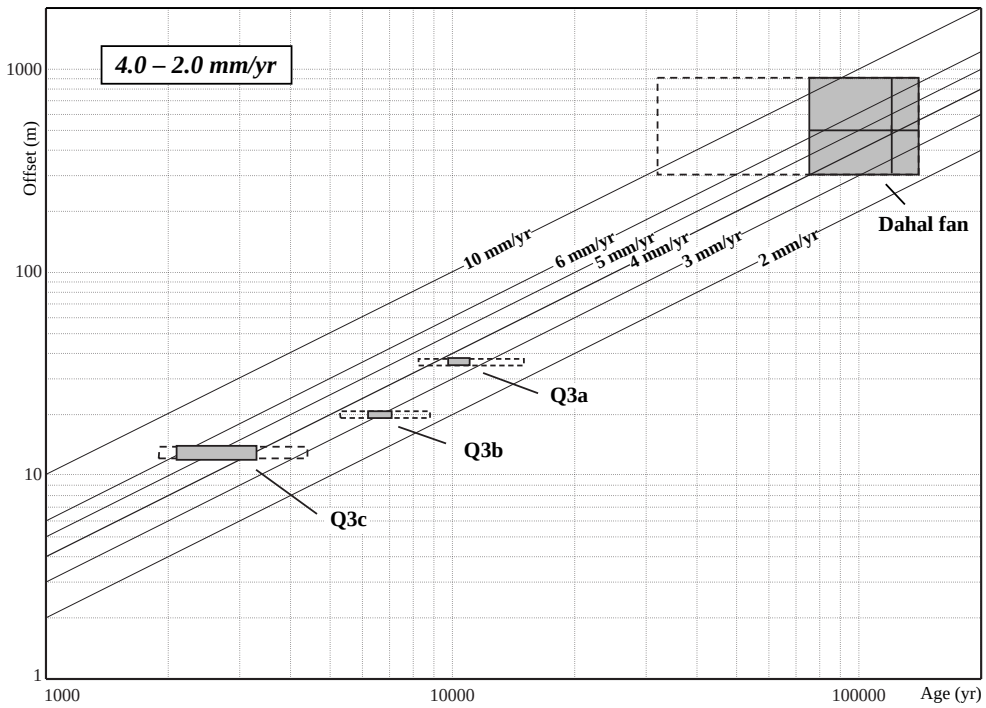

Figure 10. Constraints on the slip rate since the Pleistocene. Shaded boxes show our preferred ages and offsets. Dashed boxes indicate looser constraints due to uncertainties on the age of the El Ghor terraces. According to these data we propose a slip rate of 4 ± 2 mm yr^{-1} along the Wadi Araba. See text for detailed discussion.

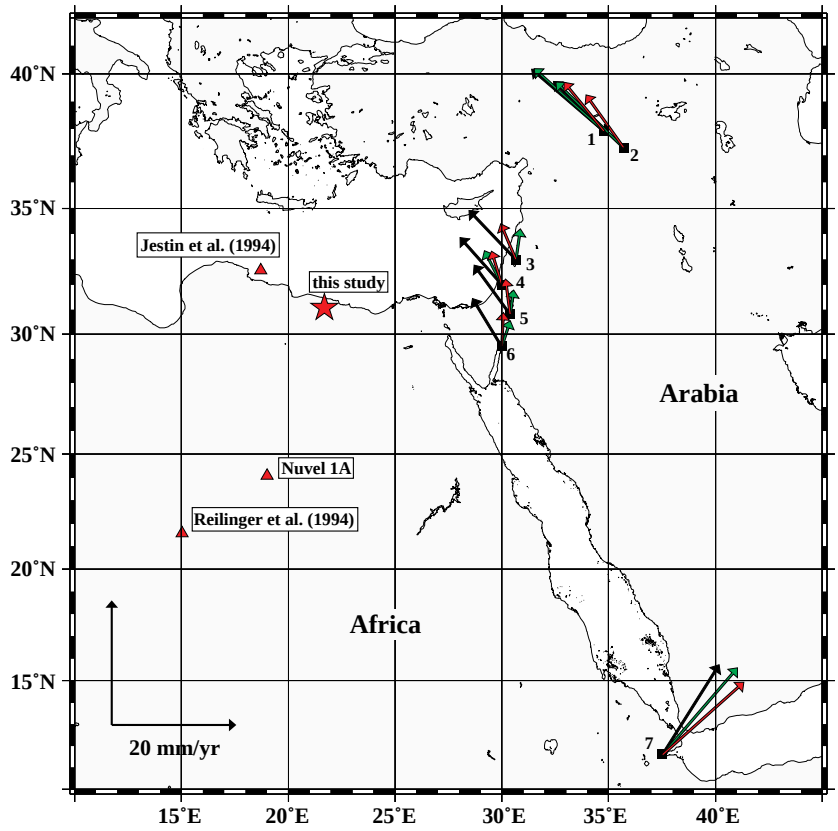

Figure 11. Location of the kinematic data listed in Table 2. The green arrows show the data we have used to compute our Eulerian pole. The red arrows show the direction and velocity at each point for our best-fitting pole (Table 3). Black arrows show the motion predicted by Nuvel1A for comparison. The location of the various Eulerian poles (describing the motion of Arabia relative to Africa) discussed in the text are also shown. The model we propose can fit the data along the Dead Sea fault, in the Caucasus (points 1 and 2) and in Asal (point 7). It does not predict compression along the Dead Sea fault, unlike Nuvel1A, and compression is not observed.

Table 2. Kinematic constraints on the motion of Arabia relative to Africa used to compute a new Eulerian pole (Fig. 11). Sinai is considered to belong to Africa.

Number	Latitude °N	Longitude °E	Kind of data	Reference
1	37.9	39.8	GPS	Reilinger *et al.* (1997)
2	37.3	40.7	GPS	Reilinger *et al.* (1997)
3	33.0	35.6	GPS	Pe'eri *et al.* (1998)
6	29.5	35.0	GPS	Pe'eri *et al.* (1998)
4	32.0	35.0	SLR	Smith *et al.* (1994)
7	11.6	42.5	morphotectonic	DeChabalier & Avouac (1994)
5	30.8	35.4	morphotectonic	this study

Table 3. Comparison between observed and predicted velocities at the various sites listed in Table 2 according to the Eulerian poles of Table 1.

Data	Slip rate obs. (mm yr^{-1})	This study	Jestin et al. (1994)	Reilinger et al. (1997)	Nuvel1A
1	15.08	10.14	11.35	14.97	14.65
2	15.21	10.38	11.76	15.10	14.77
3	5.00	6.26	8.10	11.49	10.39
4	6.10	5.60	7.70	10.84	9.60
5	4.00	5.70	8.10	10.61	9.31
6	4.40	5.50	8.20	10.02	8.59
7	18.40	17.57	21.15	15.01	16.19

ACKNOWLEDGMENTS

We benefited from helpful comments by A. Agnon. We thank P. Tapponnier and A. Cisternas for fruitful discussions. This work benefited from constructive reviews by S. Marco, T. Rockwell and K. Sieh. The work of NAK is supported by the deanship of scientific research of the University of Jordan.

REFERENCES

Begin, Z.B., Ehrlich, A. & Nathan, Y., 1974. Lake Lisan, the Pleistocene precursor of the the Dead Sea, *Israel Geol. Surv. Bull.,* **63,** 1–30.

Begin, Z.B., Broecker, W., Buchbinder, B., Druckman, Y., Kaufman, A., Magaritz, M. & Neev, D., 1985. Dead Sea and Lake Lisan levels in the last 30 000 tears: a preliminary report, *Israel geol. Rept,* **29/85**.

Ben-Avraham, Z., 1985. Structural framework of the Gulf of Elat (Aqaba), northern Red Sea, *J. geophys. Res.,* **90,** 703–726.

Ben-Menahem, A., 1981. Variation of the slip and creep along the Levant Rift over the past 4500 years, *Tectonophysics,* **80,** 183–197.

Blair, T. & McPherson, J.G., 1994. Alluvial fans and their natural distinction from rivers based on morphology, hydraulic processes, sedimentary processes, and facies asemblages, *J. sed. Res.,* **A64,** 450–489.

Bowman, D., 1988. The declining but non-rejuvanating base level—the lake Lisan, the Dead Sea area, Israel, *Earth Surf. Proc. Landforms,* **13,** 239–249.

Bowman, D. & Gross, T., 1992. The highest stand of lake Lisan, ~150 meter below MSL, *Israel J. Earth Sci.,* **41,** 233–237.

Bowman, D., 1995. Active surface ruptures on the northern Arava fault, the Dead Sea Rift, *Israel J. Earth Sci.,* **44,** 51–59.

Brook, E.J., Kurz, M.D., Eckert, R.D., Denton, G.H., Brown, E.T., Raisbeck, G.M. & Yiou, F., 1993. Chronology of Taylor glacier advances in Arena Valley, Antartica, using in situ cosmogenic ^{3}He and ^{10}Be, *Quat. Res.,* **39,** 11–23.

Brown, E.T., Bourles, D., Burchfield, B.C., Qidong, D., Jun, L., Molnar, P., Raisbeck, G.M. & Yiou, F., 1998. Estimation of slip rate in the southern Tien Shan using cosmic ray exposure dates of abandoned alluvial fans, *Geol. Soc. Am. Bull.,* **110,** 377–386.

Bull., W.B., 1964. Geomorphology of segmented alluvial fan in western Fresno County, California, *USGS Prof. Pap.,* **352-E**.

Bull., W.B., 1991. *Geomorphic Responses to Climatic Change,* Oxford University Press, Oxford.

Cerling, T.E. & Craig, H., 1994. Geomorphology and in-situ cosmogenic isotopes, *Ann. Rev. Earth planet. Sci.,* **22,** 273–317.

Courtillot, V., Armijo, R. & Tapponnier, P., 1987. The Sinai triple junction revisited, *Tectonophysics,* **141,** 151–168.

DeChabalier, J.B. & Avouac, J.P., 1994. Kinematics of the Asal Rift (Djibouti) determined from the deformation of Fieale Volcano, *Science,* **265,** 1677–1681.

DeMets, C., Gordon, R.G., Argus, D.F. & Stein, S., 1994. Effect of recent revisions to the geomagnetic reversal time scale on estimates of current plate motions, *Geophys. Res. Lett.,* **21,** 2191–2194.

Druckman, Y., Margaritz, M. & Sneh, A., 1987. The shrinking of lake Lisan, as reflected by the diagenesis of its marginal oolitic deposits, *Israel J. Earth Sci.,* **36,** 101–106.

Freund, R., Zak, I. & Garfunkel, Z., 1968. Age and rate of the sinistral movement along the Dead Sea Rift, *Nature,* **220,** 253–255.

Frumkin, A., Magaritz, M., Carmi, I. & Zak, I., 1991. The Holocene climatic record of the salt caves of Mount Sedom, Israel, *Holocene,* **1,** 191–200.

Frumkin, A., Carmi, I., Zak, I. & Magaritz, M., 1994. Middle Holocene environmental change determined from the salt caves of Mount Sedom, Israel, in *Late Quaternary Chronology and Paleoclimates of the Eastern Mediterranean*, pp. 315–332, eds Bar-Yosef, O. & Kra, R.S., American School of Prehistoric Research, Cambridge, MA.

Gardosh, M., Reches, Z. & Garfunkel, Z., 1990. Holocene tectonic deformation along the western margins of the Dead Sea, *Tectonophysics,* **180,** 123–137.

Garfunkel, Z., Zak, I. & Freund, R., 1981. Active faulting in the Dead Sea Rift, *Tectonophysics,* **80,** 1–26.

Gillespie, A. & Molnar, P., 1995. Asynchronous maximum advances of mountain and continental glaciers, *Rev. Geophys.,* **33,** 311–364.

Ginat, H., Enzel, Y. & Avni, Y., 1998. Translocated Plio-Peistocene drainage systems along the Arava fault of the Dead Sea transform, *Tectonophysics,* **284,** 151–160.

Grossman, S. & Gerson, R., 1987. Fluviatile deposits and morphology of alluvial surfaces as indicators of Quaternary environmental changes in the southern Negev, Israel, in *Desert Sediments: Ancient and Modern,* eds Frostick, L. & Ried, I., *Geol. Soc. Lond. Spec. Publ.,* **35,** 17–29.

Hall, J.K., 1994. *Digital Shaded-Relief Map of Israel and Environs,* Geol. Surv. Israel, Jersusalem, Israel.

Harden, J.W. & Matti, J.C., 1989. Holocene and late Pleistocene slip rates on the San Andreas fault in Yucaipa, California, using displaced alluvial-fan deposits and soil chronology, *Geol. Soc. Am. Bull.,* **101,** 1107–1117.

Horowitz, A., 1987. Palynological evidence for the age and rate of sedimentation along the Dead Sea Rift, and structural implications, *Tectonophysics,* **141,** 107–115.

Jestin, F., Huchon, P. & Gaulier, J.M., 1994. The Somalia plate and the Eastern Africa Rift System, present-day kinematics, *Geophys. J. Int.,* **116,** 637–654.

Joffe, S. & Garfunkel, Z., 1987. Plate kinematics of the circum Red Sea—a re-evaluation, *Tectonophysics,* **153,** 271–294.

Kaufman, A., Yechieli, Y. & Gardosh, M., 1992. Reevaluation of the lake-sediment chronology in the Dead Sea basin, Israel, based on new ^{230}Th/U dates, *Quat. Res.,* **38,** 292–304.

Klein, C., 1982. Morphologic evidence of lake level changes, western shore of the Dead Sea, *Israel J. Earth Sci.,* **31,** 67–94.

Klinger, Y., 1999. Sismotectonique de la faille du Levant, *PhD thesis*, University of Strasbourg, France.

Ku, T.L., 1976. The uranium series methods of age determination, *Ann. Rev. Earth planet. Sci.,* **4,** 347–379.

Le Pichon, X. & Gaulier, J.M., 1988. The rotation of Arabia and the Levant fault system, *Tectonophysics,* **153,** 271–294.

McKenzie, D.P., Davies, D. & Molnar, P., 1970. Plate tectonics of the Red Sea and East Africa, *Nature,* **226,** 243–248.

Mastalerz, K. & Wojewoda, J., 1993. Alluvial fan sedimentation along an active strike-slip fault; Plio-Pleistocene pre-Kaczawa fan, SW Poland, in *Alluvial Sedimentation,* eds Marzo, M. & Puigdefabregas, C., *Int. Assoc. Sed. Spec. Publ.,* **17,** 293–304.

Molnar, P. *et al.*, 1994. Quaternary climate change and the formation of river terraces across growing anticlines on the north flank of the Tien Shan, China, *J. Geol.,* **102,** 583–602.

Pe'eri, S., Wdowinski, S. & Shtivelman, A., 1998. Current plate motion across the Dead Sea fault as determined from 18 month of continuous GPS monitoring, *26th General Assembly of European Seismological Commision, Tel-Aviv, Israel (*abstract).

Peltzer, G., Tapponnier, P., Gaudemer, Y., Meyer, B., Guo, S., Yin, K., Chen, C. & Dai, H., 1988. Offsets of late Quaternary morphology, rate of slip and recurrence of large earthquakes on the Chang Ma fault (Gansu, China), *J. geophys. Res.,* **93,** 7793–7812.

Peltzer, G., Tapponnier, P. & Armijo, R., 1989. Magnitude of Late Quaternary left-lateral displacements along the north edge of Tibet, *Science,* **246,** 1285–1289.

Quennell, A.M., 1955. Geological map of Jordan, 1/250000, sheet no. 2.

Quennell, A., 1956. The structural and geomorphic evolution of the Dead Sea Rift, *Q. J. geol. Soc. Lond.,* **114,** 1–24.

Reilinger, R.E. *et al.*, 1997. Global positioning system measurements of present-day crustal movements in the Arabia-Africa-Eurasia plate collision zone, *J. geophy. Res.,* **102,** 9983–9999.

Ritz, J.F., Brown, E.T., Bourles, D.L., Philip, H., Schlupp, A., Raisbeck, G.M., Yiou, F. & Enkhtuvshin, B., 1995. Slip rates along active faults estimated with cosmic-ray-exposure dates: application to the Bogd fault, Gobi-Altai, Mongolia, *Geology,* **23,** 1019–1022.

Smith, D.E., Kolenkiewicz, R., Robbins, J.W., Dunn, P.J. & Torrence, M.H., 1994. Horizontal crustal motion in the central and eastern Mediterranean inferred from satellite laser ranging measurements, *Geophys. Res. Lett.,* **21,** 1979–1982.

Sneh, A., 1979. Late Pleistocene fan-delta along the Dead Sea rift, *J. sed. Petrol.,* **49,** 541–552.

Ten Brink, U.S., Ben-Avraham, Z., Bell, R.E., Hassouneh, M., Coleman, D.F., Andreasen, G., Tibor, G. & Coakley, B., 1993. Structure of the Dead Sea pull-apart basin from gravity analyses, *J. geophys. Res.,* **98,** 21 877–21 894.

Troeh, F.R., 1965. Landform equations fitted to contour maps, *Am. J. Sci.,* **263,** 616–627.

Yechieli, Y., Magaritz, M., Levy, Y., Weber, U., Kafri, U., Woelfli, W. & Bonani, G., 1993. Late Quaternary geological history of the Dead Sea area, Israel, *Quat. Res.,* **39,** 59–61.

Zilberman, E., 1993. The late Pleistocene sequence of the northwestern Negev flood plains—a key to reconstructing the paleoclimate of southern Israel in the last glacial, *Israel J. Earth Sci.,* **41,** 155–167.